Comparison of Polarization Diversity Configurations of SOI Strip Waveguide-Based Dual-Polarization Wavelength Conversion for S-Band Transmission

Hidenobu Muranaka
Fujitsu Limited
Kawasaki, Japan
muranaka.hide@fujitsu.com

Tomoyuki Kato
Fujitsu Limited
Kawasaki, Japan
kato.tom@fujitsu.com

Tokuharu Kimura
Fujitsu Limited
Kawasaki, Japan
kimura.tokuharu@fujitsu.com

Shun Okada
Fujitsu Limited
Kawasaki, Japan
okada.shun@fujitsu.com

Yu Tanaka
Fujitsu Limited
Kawasaki, Japan
yu_tanaka@fujitsu.com

Tsuyoshi Yamamoto
Fujitsu Limited
Kawasaki, Japan
yamamoto_tsuyo@fujitsu.com

Isaac Sackey
Fraunhofer Heinrich-Hertz-Institute
Berlin, Germany
isaac.sackey@hhi.fraunhofer.de

Gregor Ronniger
Fraunhofer Heinrich-Hertz-Institute
Berlin, Germany
gregor.ronniger@hhi.fraunhofer.de

Robert Elschner
Fraunhofer Heinrich-Hertz-Institute
Berlin, Germany
robert.elschner@hhi.fraunhofer.de

Carsten Schmidt-Langhorst
Fraunhofer Heinrich-Hertz-Institute
Berlin, Germany
carsten.schmidt-langhorst@hhi.fraunhofer.de

Colja Schuberti
Fraunhofer Heinrich-Hertz-Institute
Berlin, Germany
colja.schubert@hhi.fraunhofer.de

Takeshi Hoshida
Fujitsu Limited
Kawasaki, Japan
hoshida@fujitsu.com

***Abstract*— Using wavelength conversion of our fabricated SOI strip waveguide, we compared experimentally the polarization-insensitive configuration toward S-band real-time transmission. It is found that parallel configuration is 3dB superior in in-out conversion efficiency to loop configuration.**

Keywords*— *optical fiber communication, optical wavelength conversion, nonlinear optics, polarization diversity

I. INTRODUCTION

The capacity enlargement of optical networks becomes important with the increase of communication traffic. As one of the cost-effective means of satisfying this requirement in today's transmission systems, bandwidth expansion by multi-band transmission systems using signals other than C-band has been studied [1]. However, outside the C-band, a suitable transceiver is not available except for a part of the L-band. Therefore, we proposed the concept of multi-band system which combined the existing C-band transceiver and all-optical wavelength conversion which can simultaneously process the signal over wide wavelength range [2].

All-optical wavelength conversion is reported not only using highly nonlinear fibers but also using integrated waveguide materials [3,4]. We focus on silicon-on-insulator (SOI) waveguides and investigate the feasibility of broadband transmission with dispersion-tailored SOI waveguides by a CMOS-compatible high precision fabrication process. As a first step, we confirmed the wide-band wavelength conversion characteristics using our designed and fabricated SOI strip waveguide [5]. In addition, 32-GBd QPSK signal converted to S-band was transmitted over a 100-km standard single-mode fiber (SSMF) [6]. While the above results provide a basis for paving the way for practical wavelength converters, the polarization sensitivity of the device has been limited to single-polarization for most of the reported demonstrations [6-7]. In order to transmit an S-band signal using a C-band real-time transceiver, two wavelength conversions from the C-band to the S-band and from the S-band to the C-band, and polarization diversity configurations are required. The wavelength conversion in the SOI waveguide used in references [6-8] is without conversion back to the original C-band. As a previous study reported about polarization-diversity based wavelength conversion was not inter-band (e.g. not C-to-S) but conversion was within C-band by arranging single SOI waveguide in a loop configuration [8].

Therefore, in this paper, we compared experimentally the polarization diversity configuration when wavelength conversion is performed from the C-band to the S-band in a SOI strip waveguide for S-band signal transmission. In our previous experimental work, several waveguides were selected from our fabricated waveguides based on single polarization conversion efficiency and conversion bandwidth [9]. As a result of evaluating conversion efficiency in diversity operation by changing conditions of signal and pump light in loop and parallel configuration, it was clarified that parallel configuration was more suitable than loop configuration.

II. CHARACTERISTICS OF SOI STRIP WAVEGUIDE-BASED DUAL-POLARIZATION WAVELENGTH CONVERSION

Our experimental system is shown in Fig. 1 (a). The pump light and the C-band signal are put into the SOI strip waveguide, and converted light (i.e., idler), in the S-band, is generated by four-wave mixing (FWM). An integrated tunable laser assembly (ITLA) at a wavelength of 1527 nm is used as the pump light. The pump light is amplified by an Erbium-doped fiber amplifier (EDFA), and the intensity and polarization are adjusted by a variable optical attenuator, a

This paper is partly based on results obtained from a project carried out by Fujitsu Limited, JPNP20017, commissioned by the New Energy and Industrial Technology Development Organization (NEDO).

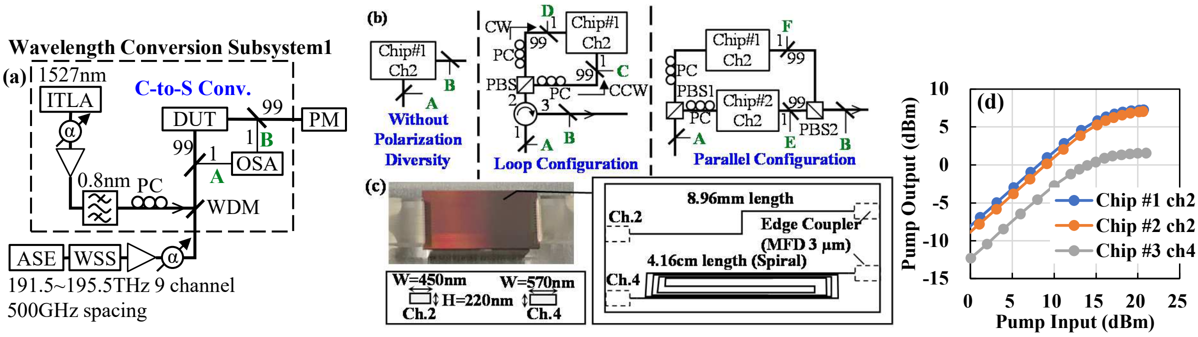

Fig.1 (a) Experimental setup for wavelength conversion evaluation of SOI waveguide; (b) Polarization diversity configuration of SOI waveguides as DUT shown in (a); (c) Photo of our fabricated chip #1 and schematic diagram of chip layout and cross-section view indicating waveguide width W and height H of 2 waveguide channels; (d) Input versus output pump power of Chip # 1 ch 2, Chip # 2 ch 2 and Chip # 3 ch 4

wavelength filter, and a polarization controller (PC). For the test signal, a C-band amplified spontaneous emission (ASE) light source and a C-band wavelength selective switch (WSS) are used to generate an unmodulated 9 wavelength-division multiplexed (WDM) channel test signal with a width of 35 GHz at 500 GHz intervals in the frequency range from 191.5 to 195.5 THz (i.e., wavelength range from 1533.47 to 1565.50 nm). In addition, the signal light is multiplexed with the pump light by a WDM coupler, but due to the operating bandwidth of the WDM coupler, the bandwidth of the signal is limited to above frequency range. Note that green letters A-F in Figs. 1 (a) and (b) are 20 dB couplers arranged as monitoring points, and tapped port is connected to either an Optical Spectrum Analyzer (OSA) or a power meter (PM). Wavelength conversion subsystem (WCS) 1 includes the pump light sources, SOI waveguide (as a nonlinear medium) with polarization diversity configuration, and a wavelength filter (not shown in Fig.1 (a)) for removing signal light and pump light after wavelength conversion. By using two WCSs, S-band optical amplifiers for compensating the losses caused by the wavelength conversion and transmission line, and C-band real-time transceivers, transmission experiments in S-band become possible. The part shown by DUT (Device Under Test) in Fig. 1 (a) represents three types of connection configurations of SOI strip waveguides for evaluating polarization diversity characteristics. Each connection configuration is shown in Fig. 1 (b). In the loop configuration, a double polarization signal enters a polarization beam splitter (PBS) via an optical circulator. The PBS splits the incoming light into two orthogonal polarizations in a clockwise (CW) and a counterclockwise (CCW) directions. Each PC in the loop is used to align both CW and CCW propagating waves to the transverse electric (TE) mode of the waveguide. After propagation of light in the CW and the CCW directions, the light waves are recombined in the PBS and collected at port 3 of the circulator. When a dual-polarization signal is coupled to a linearly polarized pump at 45 degree relative to the axis of the PBS, the pump power is equally divided in the CW and the CCW directions, and two counter-propagation co-polarized FWM processes occur in the nonlinear waveguide [8]. In the parallel configuration shown in Fig. 1 (b), after the dual polarization signal is divided into two orthogonal signal polarizations by the PBS1, each signal is input in alignment with the TE modes of the two waveguides Chip # 1 and # 2 via

TABLE1. CORRESPONDENCE OF CONNECTION BETWEEN WAVEGUIDE CHANNEL AND FIBER

Chip #	Ch.2 8.96mm length	Ch.4 4.16 cm length
# 1	Connected	Not connected
# 2	Connected	Not connected
# 3	Not connected	Connected

PCs. Although the light passing through the waveguide is recombined by another PBS2, the two optical path lengths between PBS1 and PBS2 must be aligned during signal transmission, and an optical delay line is inserted in one path (not shown in Fig. 1 (b)). In this evaluation, a total of three chips, named Chip # 1 to # 3, were used. Fig. 1 (c) shows the photograph of our fabricated chip (Chip # 1) and part of the chip layout and cross-section view indicating waveguide width W and height H of two waveguide channels, named ch 2 and ch 4. Each chip has the same layout, and a plurality of waveguide channels different in length and width are formed. An edge coupler is formed on the end face of the chip as a connection interface with the fiber. However, the channel of the waveguide to which the fiber is connected is changed for each chip, therefore the correspondence table of which chip is connected to which waveguide channel is shown in Table 1. For stable evaluation, modules with fixed fibers and waveguide were prepared for each chip. In the loop configuration, two waveguides of ch 2 and ch 4, with different lengths and widths in the loop configuration were compared. When the parallel configuration of the WCS1 is constructed, it is composed of ch 2 of two chips and evaluated. Fig. 1 (d) shows the input power dependence of the pump light of the Chip # 1 ch 2, Chip # 2 ch 2 and Chip # 3 ch 4 without polarization diversity. The insertion loss is about 8 dB for Chip # 1 ch 2, about 9 dB for Chip # 2 ch 2, and about 12.5 dB for Chip # 3 ch 4. It was confirmed that it was in the saturation region from around + 15 dBm. On the basis of this result, the polarization diversity operation was confirmed and the dependence of the conversion efficiency (CE) on the input power of the signal light was investigated by introducing the signal light at some pump light intensities. In this paper, the CE is defined by the following two indices, namely; Output CE and External CE. The Output CE is defined as the power ratio between idler and signal at output port. However, the External CE is defined as the power ratio between idler at output port and signal at input port. Since the definition of the External CE includes the input signal power, by limiting the number of WDM channels to a maximum of 9, the input signal power per WDM channel can be set high.

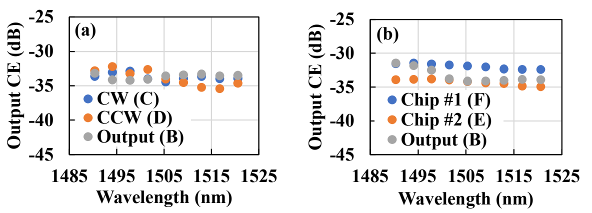

Fig.2 Conversion bandwidth of (a) loop configuration with Chip #1, (b) parallel configuration with Chip # 1 and # 2

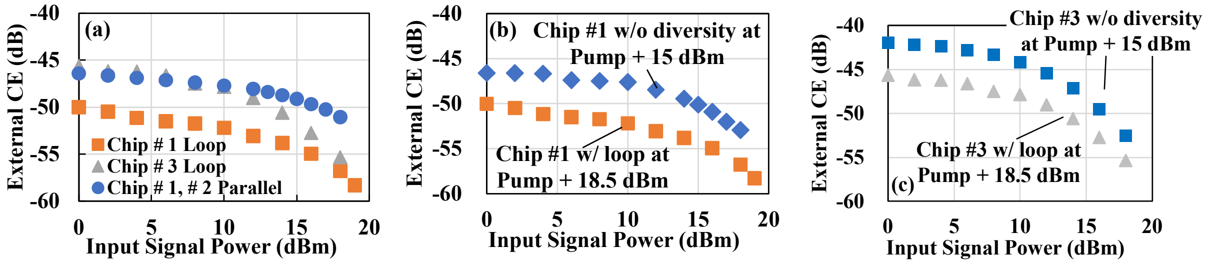

Fig.3 External conversion efficiency of (a) Chip # 1 loop, Chip # 3 loop, and Chip # 1 and # 2 parallel; without diversity at Pump + 15 dBm and with loop at Pump + 18.5 dBm of Chip (b) # 1 and (c) # 3

At first, the operation of polarization diversity was confirmed by the loop configuration of Chip # 1 and the parallel configuration of Chip # 1 and # 2. In consideration of PBS and circulator loss, the pump input set + 18.5 dBm in the loop and + 18 dBm in the parallel at the monitor A. The input signal used 9 WDM channels and was + 12 dBm total at the monitor A. The intensities of idler lights were measured by the OSA (res 0.5 nm) at the monitors C (CW), D (CCW) and B (output) in the loop configuration, and at the monitors E, F and B in the parallel configuration. The Output CE calculated from the measurement results of the OSA is shown in Fig. 2, and the loop configuration corresponds to Fig. 2 (a) and the parallel configuration corresponds to Fig. 2 (b). The horizontal axis represents the wavelength of idler light, and the wavelength conversion is confirmed in each path of both diversity configurations in a wideband of the S-band. In the loop configuration, wavelength dependence was observed in the CCW path, but the difference in Output CE between the two paths was within 2 dB, and it was confirmed that polarization diversity operation was performed. In the parallel configuration shown in Fig. 2 (b), although the wavelength dependence is smaller than that in the loop configuration, a difference of more than 2 dB is generated in the conversion efficiency in each path. Since the insertion loss of the Chip # 2 is higher than that of the Chip # 1, it is considered that the difference in the pump power at the waveguide entrance caused Output CE to decrease.

Next, the External CE in each diversity configuration with respect to the input signal power of 1 WDM channel at 192 THz under the above pump light condition was calculated. Fig. 3 (a) shows the External CE with respect to the input signal power in the loop configuration of Chip # 1, the loop configuration of Chip # 3, and the parallel configuration of Chip # 1 and # 2. It was confirmed that the loop configuration of Chip #1 is about 3 dB lower than the parallel configuration. In order to examine the effect of the loop configuration, the result of comparing the External CE with and without the loop configuration of Chip # 1 is shown in Fig. 3 (b). The plot without polarization diversity is measured with pump input of + 15 dBm at the monitor A, but the loop configuration reduces the External CE by about 3 to 4 dB. The lowering of the External CE observed in the loop configuration was also present with Chip # 3 (see Fig. 3 (c)). It is considered that this decrease in the External CE is caused mainly by the fact that when the pump and the signal input from both end faces of single waveguide in the loop configuration, two FWM occurs in opposite directions to each other, and the effective length of the waveguide is reduced by about half. In the parallel configuration, the effective length does not decrease because the pump light and the signal light are inputted from only one side of the waveguide, and both the External CE after the pump light is split by the PBS such as Fig. 3 (a) and the External CE when the pump light decreases by 3 dB without olarization diversity such as Fig. 3 (b) are almost the same. From these results, four waveguides are required for two WCSs to convert the C-band signal into the S-band and the S-band back to the C-band using the C-band real-time transceivers. From Figs. 3 (b) and 3 (c), there is a difference in the reduction of the External CE between Chip # 1 and Chip # 3 having different waveguide lengths. The External CE of Chip # 3 is higher in the low input signal power region, and greatly reduced in the high input signal power region to be approximately equal to that of Chip # 1. The decrease of the External CE in the low input signal power region may cause a small OSNR depending on the input power range of the optical amplifier after wavelength conversion. On the other hand, the lowering of the External CE in the high input signal power region has a concern of signal quality degradation. We plan to verify the effect of the signal quality by the input power in a real-time transmission experiment.

III. Conclusion

We compared experimentally two polarization diversity configurations of our fabricated SOI strip waveguides for S-band real-time transmission using dual-polarized wavelength conversion. It is clarified that the in-out conversion efficiency is reduced by about 3 dB in the loop configuration and the parallel configuration is suitable.

References

[1] A. Napoli, *et al.*, "Towards multiband optical systems," in Advanced Photonics 2018 (BGPP, IPR, NP, NOMA, Sensors, Networks, SPPCom, SOF), OSA Technical Digest (online) (Optica Publishing Group, 2018), paper NeTu3E.1.

[2] T. Kato, *et al.*, "Real-time transmission of 240×200-Gb/s signal in S+C+L triple-band WDM without S- or L-band transceivers," ECOC2019, PD1.7, 2019.

[3] T. Kobayashi, *et al.,* "Wide-band inline-amplified WDM transmission using PPLN-based optical parametric amplifier," J. Lightw. Technol., vol. 39, no. 3, pp. 787–794, Feb. 2021.

[4] F. Da Ros, *et al.,* "Characterization and optimization of a high-efficiency AlGaAs-on-Insulator-based wavelength converter for 64- and 256-QAM signals," J. Lightwave Technol. 35, 3750–3757 (2017).

[5] H. Muranaka, *et al.*, " Characterization of Dispersion-Tailored Silicon Strip Waveguide for Wideband Wavelength Conversion," OECC/PSC2022, Tu4D.2.

[6] I. Sackey, *et al.*, "Ultra-wideband All-optical Interband Wavelength Conversion Using a Low-complexity Dispersion-engineered SOI Waveguide," ECOC2022, Tu2F.3.

[7] R. Adams, *et al.*, "Wavelength conversion of 28 GBaud 16-QAM signals based on four-wave mixing in a silicon nanowire," Optics Express, Vol. 22, no.4, pp.4084-4090, Feb. 2014.

[8] F. Da. Ros, *et al.*, " Dual-polarization wavelength conversion of 16-QAM signals in a single silicon waveguide with a lateral p-i-n diode," Photo. Research, Vol. 6, no.5, pp. B.23-B.29, Apr. 2018.

[9] H. Muranaka, *et al.*, "Design and Characterization of Dispersion-Tailored Silicon Strip Waveguides toward Wideband Wavelength Conversion," in press.